Naphthalene-Derived Secondary Organic Aerosols Interfacial Photosensitizing Properties

X. Wang, R. Gemayel, V. Baboomian, K. Li, A. Boreave, C. Dubois, S. Tomaz, S. Perrier, S. Nizkorodov, C. George

Naphthalene-derived secondary organic aerosols interfacial photosensitizing properties

Xinke Wang[1], Rachel Gemayel[1], Vahe J. Baboomian[2], Kangwei Li[1], Antoinette Boreave[1], Clement Dubois[1], Sophie Tomaz[1], Sebastien Perrier[1], Sergey A. Nizkorodov[2], Christian George[1,*]

[1]Univ Lyon, Université Claude Bernard Lyon 1, CNRS, IRCELYON, F-69626, Villeurbanne, France.

[2]Department of Chemistry, University of California, Irvine, Irvine, California, 92697, USA.

[*]To whom correspondence should be addressed. Email: christian.george@ircelyon.univ-lyon1.fr

Key points

- Naphthalene-derived SOA contains oxygenated aromatic compounds with photosensitizing properties.
- Photosensitized oxidation of d-limonene and β-pinene by naphthalene-derived SOA results in particle growth.
- Sulfate is formed through both dark and photosensitized chemical reactions between naphthalene-derived SOA and SO_2.

Abstract

We investigated the photosensitizing properties of secondary organic aerosol (SOA) formed during the hydroxyl radical (OH) initiated oxidation of naphthalene. This SOA was injected into an aerosol flow tube and exposed to UV radiation and gaseous volatile organic compounds or sulfur dioxide (SO_2). The aerosol particles were observed to grow in size by photosensitized uptake of d-limonene and β-pinene. In the presence of SO_2, a photosensitized production (0.2-0.3 $\mu g\ m^{-3}\ h^{-1}$) of sulfate was observed at all relative humidity (RH). Some sulfate also formed on particles in the dark, probably due to the presence of organic peroxides. The dark and photochemical pathways exhibited different trends with RH, unravelling different contributions from bulk and surface chemistry. As naphthalene and other polycyclic aromatics are important SOA precursors in the urban and suburban areas, these dark and photosensitized reactions are likely to play an important role in sulfate and SOA formation.

Plain Language Summary

Organic compounds and sulfate anions are important components of atmospheric fine particles, which play an important role in air quality, visibility, climate, as well as human and ecosystem health. Photosensitized chemistry, which is driven by reactions of electronically excited organic molecules, is a proposed pathway for fine particle growth, producing highly oxygenated compounds and sulfate anions from gaseous volatile organics and sulfur dioxide, a key air pollutant. Aromatic hydrocarbons and their oxidation products are important components of fine particles in urban environments. This work shows that fine particles formed by oxidation of naphthalene, a common aromatic hydrocarbon, possess photosensitizing properties making them efficient catalysts for atmospheric oxidation of sulfur dioxide and volatile organics.

1. Introduction

Organic compounds and sulfate anions are ubiquitous in ambient aerosols, accounting for 20-90% and 10-60% of the fine particulate mass, respectively (Jimenez et al., 2009; Kanakidou et al., 2005). A large fraction of these organic compounds and sulfate are secondary in nature, i.e., they are produced through atmospheric oxidation of volatile organic compounds (VOCs) (Hallquist et al., 2009) and sulfur dioxide (SO_2) (Eatough et al., 1994; Saxena & Seigneur, 1987). Both sulfate and secondary organic aerosol (SOA) significantly impact air quality, climate, as well as human and ecosystem health (Fuzzi et al., 2015; Nel, 2005). Despite extensive research spanning nearly a century, we still do not fully understand all possible pathways for their formation and transformation in the atmosphere (Zhang et al., 2007; Wang et al., 2014).

Many previous studies showed that photosensitized chemistry may be an important pathway for promoting the oxidation of VOCs (Kaur et al., 2019; Li et al., 2019a) in atmospheric particles, which can increase the mass of SOA. For example, irradiation of imidazole-2-carboxaldehyde (IC) and humic acid in the presence of various gaseous VOCs, such as d-limonene, has been shown to produce highly oxygenated compounds and thereby initiate aerosol growth by photosensitized mechanisms (Aregahegn et al., 2013; González Palacios et al., 2016; Rossignol et al., 2014; Tsui et al., 2017; Monge et al., 2012). Previous studies have suggested that the photosensitized chemistry of humic-like substances (HULIS) is not fast enough to compete with the conventional free-radical-driven growth under ambient concentrations of d-limonene (Fankhauser et al., 2020). However, while not being a major growth pathway of aerosols, photosensitized processes have the potential to change the particle phase oxidation capacity. For instance, significant amounts of oxygenated molecules with low-volatility have been observed during photosensitized oxidation of some VOCs (Smith et al., 2014; Rossignol et al., 2014; Yu et

al., 2014). The importance of such processes is obviously linked to the concentration of triplet state in the condensed phase as underlined by Kaur et al. (2019), who pooled all active triplet state into a one single T* family. In other words, in contrast to well identified radicals (such as OH), the key feature of tropospheric photosensitization is related to numerous compounds with diverse sources. Understanding those is therefore key. To further illustrate this potential importance, it has been shown that photosensitized chemistry involving the humic fraction of aerosols during Chinese haze events can explain a significant fraction of the observed sulfate formation (Wang et al., 2020a). The authors highlighted the specific role played by biomass burning (for cooking and heating during the cold season) as the main source of the aerosol's photosensitizing properties.

Naphthalene, emitted primarily from fossil fuel combustion and biomass burning, represents the smallest, most volatile, and most abundant polycyclic aromatic hydrocarbon (PAH) in the atmosphere (Zhang et al., 2012). Naphthalene is ubiquitous in suburban and urban areas, with a median concentration of 0.94 μg m^{-3} in 11 U.S. cities (Sudakin et al., 2011). The OH-initiated oxidation of naphthalene produces a number of different oxygenated compounds with high molecular weight and low-volatility, which can partition into particles and contribute to SOA mass (Chan et al., 2009; Kautzman et al., 2010; Riva et al., 2015). Naphthoquinone, a naphthalene oxidation product (McWhinney et al., 2013), is commonly found in atmospheric aerosols (e.g., Shanghai, China (Wang et al., 2017); Tempe, USA (Delhomme et al., 2008); Kurashiki City, Japan (Oda et al., 2001); Yangtze River channel (Wang et al., 2020b)), and is known to be an efficient photosensitizer, inducing redox chemistry or producing reactive oxygen species (De Lucas et al., 2014; McNeill & Canonica, 2016). SOA derived from oxidation of naphthalene under high-NO_x conditions has been shown to be weakly fluorescent (Lee et al., 2014), resilient to photobleaching (Aiona et al., 2018), efficient in photosensitizing singlet oxygen in aqueous solutions (Manfrin et

al., 2019), capable of photosensitized oxidation of halide ions (Gemayel et al., 2021), and moderately effective in photosensitized oxidation of d-limonene (Malecha & Nizkorodov, 2017). It is therefore likely that aerosol particles containing naphthalene oxidation products (as well as oxidation products of PAHs in general) contribute to photosensitized chemistry in the atmosphere.

In this study, we investigated the photosensitizing activity of naphthalene-derived SOA using both gaseous VOCs and SO_2 as reaction partners. The naphthalene-derived SOA was generated in a laminar-flow Gothenburg (Go:PAM) oxidation flow reactor, then its photosensitizing properties were investigated by explicitly measuring particle growth in aerosol flow tube (AFT) experiments, in which particles were exposed to near-UV radiation in presence of VOCs or SO_2. Our data suggests that these aerosols do indeed exhibit photosensitized chemistry, by converting SO_2 into sulfate and d-limonene and β-pinene into particle-phase organic products.

2. Materials and Method

As shown in Figure 1, the experimental setup mainly consisted of a Go:PAM oxidation flow reactor and an aerosol flow reactor.

2.1 Go:PAM Description

The Go:PAM flow reactor (9.6 cm inner diameter, 100 cm length) is made of quartz glass and surrounded by two 30 W Philips ultraviolet lamps capable of producing 254 nm radiation (Watne et al., 2018). The gas flow injected into the Go:PAM chamber consisted of 250 mL min^{-1} of pure air bubbled through hydrogen peroxide (H_2O_2, Sigma Aldrich, 26.4 wt. % in H_2O) solution, 20 mL min^{-1} of pure air containing naphthalene (Sigma Aldrich, 99%) vapor, 1 L min^{-1} of humidified air, and 2.78 L min^{-1} of dry air, leading to a residence time of 1.8 min. The Go:PAM was operated at room temperature in the range of 297±2 K, whilst a fan was used to homogenize and maintain the

temperature. As calculated under the above conditions, the relative humidity (RH) and the concentrations of H_2O_2 and naphthalene in the Go:PAM reactor were around 29%, 5.2×10^3 ppb, and 5.5×10^2 ppb, respectively. The collection and analysis of naphthalene-derived SOA and its chemical characteristics are described in Supporting Information Texts S1-S2.

2.2 Aerosol Flow Tube Experiment

The naphthalene-derived SOA air-flow was controlled by a needle valve and sent into a charcoal denuder (100-160 mL min^{-1}) (Sigma Aldrich, Norit RBAA-3) to reduce concentrations of gaseous compounds and then into a differential mobility analyzer (DMA, TSI model 3081, impactor size 0.0508 cm) to produce monodispersed particles of desired size (mobility-equivalent diameter). The size selection by DMA further reduced the concentration of gaseous compounds in the flow. The size-selected SOA and VOC or SO_2 (Linde, France) were injected into a temperature-controlled horizontal jacketed aerosols flow tube (AFT) (6 cm internal diameter, 180 cm length) made of Pyrex (Wang et al., 2020a). In order to reduce the evaporative loss of the naphthalene-SOA particles that is known to happen after size selection (Li et al., 2019b; Yli-Juuti et al., 2017), the temperature inside the AFT was kept at 285 K. The RH inside the AFT was calculated based on the measured temperature and RH of the aerosol flow upon exiting the AFT. The AFT was surrounded by eight UV-lamps (Cleo, Philips, Netherlands) with a continuous emission spectrum over 300-420 nm and a total irradiance of 6×10^{15} photon cm^{-2} s^{-1} (Dupart et al., 2012).

As shown in Figure 1, the aerosol flow was diluted by a factor of ~2 with pure air before being sent to a scanning mobility particle sizer (SMPS, TSI 3936, impactor size 0.071 cm), an SO_2 analyzer (Thermo 43i) and an Aerodyne compact time-of-flight (cTOF) aerosol mass spectrometer (AMS), to characterize the particle size distributions in the range of 15-700 nm, gaseous SO_2 concentration, and particle-phase sulfate production, respectively. The diluted aerosol flow was

133 further diluted with pure air before being analyzed by a stander SO_2 analyzer. More details about
134 the SMPS and AMS measurements are provided in the Supporting Information section (Text S3).
135 In some experiments, a selected VOC was continuously injected in the AFT together with the
136 particles. For this purpose, a permeation tube placed in a temperature controlled oven (Dynacal,
137 Valco Instruments Co. Inc., U.S., using VICI Metronics, U.S., Dynacalibrator, model 150) was
138 used to generate a specific concentration of d-limonene or β-pinene (Rossignol et al., 2014). A
139 high-resolution proton-transfer-reaction time-of-flight mass spectrometer (PTR-TOF-MS 8000,
140 Ionicon Analytik) was then used to measure their concentrations. The detailed setup and calibration
141 of the PTR-MS were described in a previous study (Kalalian et al., 2020).

142 **3. Results and Discussion**

143 In previously published control experiments, only one VOC or SO_2 was injected into the AFT
144 (without naphthalene-derived SOA) under similar conditions to other experiments (i.e., the same
145 RH, UV exposure, temperature, and residence time). During these experiments, no loss of VOC or
146 SO_2 and no particle formation were observed (Aregahegn et al., 2013), indicating that gas-phase
147 oxidation of the VOC or SO_2 was not taking place in the AFT, due to an absence of gaseous oxidants.

148 In the first series of experiments, naphthalene-derived SOA (~5700 particles cm^{-3}, median
149 size ~46 nm) and SO_2 (1 ppm after dilution) were injected into the AFT with a residence time of
150 16 min at a high RH of 86-90%. Figure 2A shows a typical profile for the evolution of the median
151 and mean diameters of the particles at the outlet of the AFT. Notably, both the median and mean
152 diameters of particles (before UV irradiation) were smaller than selected inlet sizes, indicating
153 some particle evaporation in the first DMA and AFT. A small particle growth was observed once
154 the UV lights were switched on, growing 2 nm in terms of median and mean diameters. In addition,
155 the Diameter Growth Factor (DGF (%) = $((Dp - Dp_0)/ Dp) \times 100$) was calculated for different

156 experimental conditions (see Table 1). As RH decreases to 61-65% and 40-43%, the particle size
157 measurements indicate particle shrinking instead of growth when naphthalene-derived SOA were
158 exposed to 1 ppm SO_2 and UV irradiation. This is likely due to the particle phase undergoing
159 photodegradation when exposed to UV irradiation, resulting in smaller particle sizes. Indeed, it has
160 been shown that the photodegradation of SOA particles could produce small oxygenated VOCs
161 evaporating to the gas phase (Malecha & Nizkorodov, 2016, 2017; Wong et al., 2015). Notably, at
162 RH 40-49%, the DGF was even lower when SOA particles were exposed to SO_2 compared to
163 control experiments, possibly due to the more acidic aerosol phase enhancing the evaporation of
164 small organic acids from particles. Slade et al. (2017) suggested that degradation of SOA under
165 viscous conditions (i.e., low RH), where diffusion into the bulk is prevented, tends to promote the
166 production of multiple generations of oxidation of the same molecule, resulting in fragmentation
167 and evaporation. Such processes could also be occurring in our experiments at low RH when SO_2
168 is present.

169 In the second series of experiments, 100 nm naphthalene-derived SOA particles, up to 6000
170 particles cm^{-3}, were size-selected and exposed to 0.8 ppm SO_2 for sulfate production measurement
171 experiments. The particle size-selection was changed (from 46 to 100 nm) due to the low
172 transmission efficiency of the cTOF-AMS for particles less than 60 nm. The total amount of all
173 sulfate was then monitored (the cTOF instrument has limited capabilities to distinguish between
174 the inorganic and organic sulfate). Figure 2B shows that at different RHs, particulate sulfate was
175 produced from both dark and photosensitized chemistry. The dark production of particulate sulfate
176 can be explained by a couple of factors. Firstly, organic peroxides were found to account for ~26.2%
177 of the total naphthalene-SOA mass (Kautzman et al., 2010), which are believed to oxidize SO_2 to
178 sulfate and organosulfates (Wang et al., 2019; Yao et al., 2019; Ye et al., 2018a). In addition,

dissolved S(IV) may react with aldehydes and quinones in naphthalene-derived SOA (Kautzman et al., 2010) to produce organosulfonates (LuValle, 1952; Olson & Hoffmann, 1989). All these pathways could contribute to the measured sulfate in the dark, which are in the range of 0.003-0.11 $\mu g\ m^{-3}$. In addition, a previous study showed that the sulfate production from the reaction between SO_2 and α-pinene-derived SOA exhibits an exponential dependence on RH (Yao et al., 2019), which is similar to the result obtained in the present study (Figure 2B).

When the UV lights were switched on, 0.05-0.08 $\mu g\ m^{-3}$ of sulfate (i.e., 0.2-0.3 $\mu g\ m^{-3}\ h^{-1}$) were produced at all RHs (Figure 2B). However, although the total sulfate production increases as the RH increases, the sulfate production attributable to the photosensitized oxidation at RH 81-84% is the lowest. This indicates a more complex RH dependence on the photochemical mechanism. Saukko et al. (2012) have investigated the physical phase state (solid, semi-solid, or liquid) of SOA derived from various precursors by measuring their bounce behavior after inertial impaction on a solid substrate. The measured bounce fraction was evaluated as a function of RH and SOA oxidation level (O / C). In the case of naphthalene-derived SOA, the bounce factor was indicative of an amorphous solid or semi-solid state, up to RH close to 70%. At greater RH values, this factor decreased, indicating a phase change with particles having a less viscous, more "liquid-like" material. These trends are to be compared with the data shown in Figure 2B, where the dark chemistry was predominant only at high RH. Such chemistry could be driven, among other factors, by the peroxide, aldehyde, and quinone (i.e., naphthoquinone) compounds present in such particles (Kautzman et al., 2010) forming organosulfates, organosulfonates and sulfate (LuValle, 1952; Olson & Hoffmann, 1989; Wang et al., 2019; Yao et al., 2019; Ye et al., 2018a). But the fact that it occurs more efficiently at high RH (i.e., on more liquid particles), points towards a bulk process where the chemistry occurs after solubilization of the incoming SO_2 molecules. In addition, the

sulfate formed from dark chemistry can also impact physical properties such as hygroscopicity, acidity, and phase state (Hodas et al., 2015; Saukko et al., 2012), which may further influence the solubility of S(IV) in the aerosol phase.

In contrast, the photochemical fraction of sulfate production is reduced at higher RHs but gains in importance at low RH, where potentially the surface, or a small shell close to the surface, is available for reaction. Notably, the previous studies showed that in-particle diffusion is not rate-limiting to SO_2 uptake by α-pinene-derived SOA at low RH (<10%), whilst toluene-derived SOA starts to lose the resistance above 20% RH (Yao et al., 2019; Ye et al., 2016, 2018b). Therefore, a significant diffusion limitation is not expected in the present study. Besides, SO_2 could also be excited into the triplet state (i.e., SO_2) by direct absorption of light with wavelength from 240 to 330 nm, which could react with H_2O to produce sulfate (Kroll et al., 2018; Martins-Costa et al., 2018). However, this sulfate formation pathway was shown to be minor significant in our AFT system due to the weak overlap of SO_2 light absorption and spectral irradiance of our lamps (Wang et al., 2020a). Additionally, the bulk chemistry may also consume the existing photosensitizers and explain the reduced fraction of photochemically produced sulfate at high RHs. Thus, at higher RHs sulfate production is dominated by bulk phase solubilization and subsequent oxidation of SO_2, whereas photosensitized oxidation at the surface of the particles dominates at lower RHs.

It is notable that the mean particle size of SOA decreased from 93 nm to 85 nm as the RH increased from 37-39% to 81-84% in the dark, possibly due to the moisture-induced changes in SOA morphology or phase and high evaporation of SOA at high RH (Li et al., 2019b; Wilson et al., 2015; Wong et al., 2015; Yli-Juuti et al., 2017), reducing the surface area and volume by ~16% and ~24%, respectively. Figures 2C and 2D show that sulfate production decreases as the light intensity and SO_2 concentration decrease.

Traditionally, SO_2 oxidation is known to be mainly driven by gas-phase reactions with OH radicals, ozone, H_2O_2, nitrogen dioxide (NO_2), and transition-metal ions in the aqueous phase (Cheng et al., 2016), whilst interfacial SO_2 oxidation on acidic microdroplets (Hung & Hoffmann, 2015) and SO_2 triplet state chemistry (Kroll et al., 2018; Martins-Costa et al., 2018) were also suggested to play a role in the sulfate formation. However, the photosensitized oxidation of SO_2 has recently been discussed as an important contributor to sulfate formation on biomass burning type particles (Wang et al., 2020a). Our findings here now extend such observations also to more anthropogenic particles and are posing the question whether such photosensitized processes are widespread.

To test whether these particles exhibit photosensitized reactivity toward different partner molecules, we also exposed them to gaseous d-limonene or β-pinene. Control experiments using seed particles containing only ammonium sulfate or ammonium sulfate/succinic acid exposed to limonene and UV light did not lead to particle growth (Aregahegn et al., 2013; Monge et al., 2012). In contrast, as shown in Figure 3 and Table 1, the particle size of naphthalene-derived SOA particles (starting diameter of 37 nm) in the presence of 0.1 ppm limonene increased by 50.8% and 58.7% at RH 39-43% and 84-88%, respectively, corresponding to a residence time of 25 min. This is a remarkable amount of growth, implying that particle volume goes up by $(2.0\text{-}2.5)^3$ or by a factor of 8-16. In addition, the reaction with 0.8 ppm β-pinene at RH 45-47% and 85-89% resulted in similarly large DGFs of 8.9% and 24.2%. The RH dependence of particle growth is mainly driven by the enhanced solubility of naphthalene-derived SOA (Yao et al., 2019). Such experiments are meant to show that these particles are reactive toward unsaturated VOCs (Aregahegn et al., 2013; Monge et al., 2012), since d-limonene was found to be a more efficient SOA precursor compared to β-pinene, but are not meant to suggest a strong involvement in particle growth in the

ambient atmosphere (due to the unrealistic experimental conditions). Similar to the study of Aregahegn et al. (2013), such growth is probably caused by the formation of highly oxygenated products through limonene or β-pinene reacting with the triplet state of the photosensitizers (Monge et al., 2012; Rossignol et al., 2014).

For example, the excited photosensitizer can abstract a hydrogen from an organic molecule (i.e., d-limonene or β-pinene), through either a direct transfer or proceed via an electron transfer followed by a proton transfer (Rossignol et al., 2014). Since the initial step triggering the photosensitized uptake is a H-abstraction reaction (and not an addition to a double bond), VOCs having weak C-H bonds will react faster, which is observed here for limonene. The reduced photosensitizer radical can be oxidized to the original ground state in the presence of O_2, at the same time, producing superoxide radicals ($HO_2^{\cdot}/O_2^{\cdot-}$) (Aregahegn et al., 2013). The photoproduct VOC and photosensitizer radicals can further react with other molecules or be oxidized by HO_2 or O_2, to produce new products. The study of Rossignol et al. (2014) found that highly oxygenated organic compounds including compounds retaining the same number of carbons as d-limonene were produced from the reaction of the IC triplet state and d-limonene in the aerosol phase through ring-opening and intramolecular isomerization during the limonene oxidation process.

Interestingly, both naphthalene-derived SOAs and seed particles containing photosensitizers grow efficiently even at low RH when exposed to limonene and β-pinene VOCs (Table 1) (Aregahegn et al., 2013; Monge et al., 2012). This indicates that the photosensitized processes may occur at the surface and be sustained even on solid or semi-solid particles without passivation. This is in contrast to the expected behavior of a solid where it is expected that the high viscosities promote radical recombination and the surface is expected to be rapidly passivated. It is beyond the capabilities of these experiments to unravel the molecular reason for this observation,

but one could speculate that the presence of a photochemically active surface may locally change the nature of the surface or induce chain reactions that may propagate some surface reactivity. Another possibility is the triplet state of these photoactive compounds convert molecular oxygen into reactive oxygen (e.g., O_2^- or $^1O_2$) sustaining surface reactivity, which would be in agreement with high $^1O_2$ yield from naphthalene-SOA in aqueous solutions (Manfrin et al., 2019). The produced oxygenated VOC may also form a new phase beneath the surface, thus keeping the surface open for more reactions. This type of liquid-liquid phase separation has been observed for various SOA types even under lower RH conditions observed here (Huang et al., 2021). Whatever the underlying reason, these observations tend to support that the surface of such solid or semi-solid particles will not passivate while being illuminated with actinic light.

Notably, the increased DGF under high RH conditions indicates that the underlying photochemical mechanisms are different for the VOCs and for SO_2. Wang et al. (2020a) suggested a direct reaction of SO_2 with the organic triplet states through different pathways, possibly influenced by pH. On the other hand, Rossignol et al. (2014) suggested that the underlying mechanism for the VOC uptake is H abstraction followed by the production of multiple generation multiple products (by condensed phase autooxidation). As previously mentioned, at low RH, these first-generation products are concentrated at the surface (because they cannot diffuse to the bulk under highly viscous conditions) where they remain fully exposed to oxidants and undergo rapid further oxidation and fragmentation, yielding highly-oxygenated products with lower molar mass. Those may therefore degas (or desorb) preferably at low RH compared to high RH where diffusion into the bulk is possible. Therefore, the different trends between the VOCs and SO_2 is possibly to a combination of mass transport limitations, and different chemistries being influenced by pH.

4. Conclusions

Naphthalene is ubiquitous in suburban and urban areas and its OH radical driven oxidation produces oxygenated aromatic compounds with low volatility forming secondary organic aerosols. Those particles are found to be reactive in the dark toward SO_2 where the reaction of dissolved S(IV) with naphthalene oxidation products such as quinones, aldehydes, and organic peroxides are expected to produce organosulfonates, organosulfates and sulfates. The dark production of sulfate was observed to increase at high humidity and hence on liquid like particles. In addition, these particles possess photosensitizing properties at lower humidity (< 70% RH), and can oxidize SO_2 even on solid or semi-solid particles. Moreover, the particle size of naphthalene-derived SOA grows efficiently under irradiation in the presence of VOCs, especially d-limonene. As the RH increases, the photosensitized particle growth becomes more efficient. These results indicate that the formation of sulfate and oxygenated organic compounds through naphthalene-derived SOA photoinduced reactions contribute to the sulfate concentration and size/mass of SOA particles.

Declaration of Competing Interest

The authors declare no conflict of interest.

Acknowledgments

This project was supported by the ANR-RGC programme (project ANR-16-CE01-0013, A-PolyU502/16), and the European Union's Horizon 2020 research and innovation program under grant agreement No. 690958 (MARSU). VJB and SAN were supported by US National Science Foundation grant AGS-1853639. The data presented in this manuscript could be downloaded at https://osf.io/52ef9/.

References

Aiona, P. K., Luek, J. L., Timko, S. A., Powers, L. C., Gonsior, M., & Nizkorodov, S. A. (2018). Effect of Photolysis on Absorption and Fluorescence Spectra of Light-Absorbing Secondary Organic Aerosols. *ACS Earth and Space Chemistry*, *2*(3), 235–245. https://doi.org/10.1021/acsearthspacechem.7b00153

Allan, J. D., Bower, K. N., Coe, H., Boudries, H., Jayne, J. T., Canagaratna, M. R., et al. (2004). Submicron aerosol composition at Trinidad Head, California, during ITCT 2K2: Its relationship with gas phase volatile organic carbon and assessment of instrument performance. *Journal of Geophysical Research D: Atmospheres*, *109*(23), 1–16. https://doi.org/10.1029/2003JD004208

Aregahegn, K. Z., Nozière, B., & George, C. (2013). Organic aerosol formation photo-enhanced by the formation of secondary photosensitizers in aerosols. *Faraday Discussions*, *165*, 123–134. https://doi.org/10.1039/c3fd00044c

Canonica, S., Jans, U. R. S., Stemmler, K., & Hoigne, J. (1995). Transformation Kinetics of Phenols in Water: Photosensitization. *Environmental Science & Technology*, *29*(7), 1822–1831.

Chan, A. W. H., Kautzman, K. E., Chhabra, P. S., Surratt, J. D., Chan, M. N., Crounse, J. D., et al. (2009). Secondary organic aerosol formation from photooxidation of naphthalene and alkylnaphthalenes: Implications for oxidation of intermediate volatility organic compounds (IVOCs). *Atmospheric Chemistry and Physics*, *9*(9), 3049–3060. https://doi.org/10.5194/acp-9-3049-2009

Cheng, Y., Zheng, G., Wei, C., Mu, Q., Zheng, B., Wang, Z., et al. (2016). Reactive nitrogen chemistry in aerosol water as a source of sulfate during haze events in China. *Science Advances*, *2*(12), e1601530. https://doi.org/10.1126/sciadv.1601530

Delhomme, O., Millet, M., & Herckes, P. (2008). Determination of oxygenated polycyclic aromatic hydrocarbons in atmospheric aerosol samples by liquid chromatography-tandem mass spectrometry. *Talanta*, *74*(4), 703–710. https://doi.org/10.1016/j.talanta.2007.06.037

Dupart, Y., King, S. M., Nekat, B., Nowak, A., Wiedensohler, A., Herrmann, H., et al. (2012). Mineral dust photochemistry induces nucleation events in the presence of SO2. *Proceedings of the National Academy of Sciences*, *109*(51), 20842–20847. https://doi.org/10.1073/pnas.1212297109

Eatough, D. J., Caka, F. M., & Farber, R. J. (1994). The Conversion of SO2 to Sulfate in the Atmosphere. *Israel Journal of Chemistry*, *34*(3–4), 301–314. https://doi.org/10.1002/ijch.199400034

Fankhauser, A. M., Bourque, M., Almazan, J., Marin, D., Fernandez, L., Hutheesing, R., et al. (2020). Impact of Environmental Conditions on Secondary Organic Aerosol Production from Photosensitized Humic Acid. *Environmental Science & Technology*, *54*(9), 5385–5390. https://doi.org/10.1021/acs.est.9b07485

Fuzzi, S., Baltensperger, U., Carslaw, K., Decesari, S., Denier Van Der Gon, H., Facchini, M. C., et al. (2015). Particulate matter, air quality and climate: Lessons learned and future needs. *Atmospheric Chemistry and Physics*, *15*(14), 8217–8299. https://doi.org/10.5194/acp-15-8217-2015

Gemayel, R., Emmelin, C., Perrier, S., Tomaz, S., Baboomian, V. J., Fishman, D. A., et al. (2021). Quenching of ketone triplet excited states by atmospheric halides. *Environmental Science: Atmospheres*, *1*(1), 31–44. https://doi.org/10.1039/d0ea00011f

González Palacios, L., Corral Arroyo, P., Aregahegn, K. Z., Steimer, S. S., Bartels-Rausch, T., Nozière, B., et al. (2016). Heterogeneous photochemistry of imidazole-2-carboxaldehyde: HO2 radical formation and aerosol growth. *Atmospheric Chemistry and Physics*, *16*(18), 11823–11836. https://doi.org/10.5194/acp-16-11823-2016

Hallquist, M., Wenger, J. C., Baltensperger, U., Rudich, Y., Simpson, D., Claeys, M., et al. (2009). The formation, properties and impact of secondary organic aerosol: Current and emerging issues. *Atmospheric Chemistry and Physics*, *9*(14), 5155–5236. https://doi.org/10.5194/acp-9-5155-2009

Hodas, N., Zuend, A., Mui, W., Flagan, R. C., & Seinfeld, J. H. (2015). Influence of particle-phase state on the hygroscopic behavior of mixed organic-inorganic aerosols. *Atmospheric Chemistry and Physics*, *15*(9), 5027–5045. https://doi.org/10.5194/acp-15-5027-2015

Huang, G., Liu, Y., Shao, M., Li, Y., Chen, Q., Zheng, Y., et al. (2019). Potentially Important Contribution of Gas-Phase Oxidation of Naphthalene and Methylnaphthalene to Secondary Organic Aerosol during Haze Events in Beijing. *Environmental Science and Technology*, *53*(3), 1235–1244. https://doi.org/10.1021/acs.est.8b04523

Huang, Y., Mahrt, F., Xu, S., Shiraiwa, M., Zuend, A., & Bertram, A. K. (2021). Coexistence of three liquid phases in individual atmospheric aerosol particles. *Proceedings of the National Academy of Sciences*, *118*(16), e2102512118. https://doi.org/10.1073/pnas.2102512118

Hung, H. M., & Hoffmann, M. R. (2015). Oxidation of Gas-Phase SO2 on the Surfaces of Acidic Microdroplets: Implications for Sulfate and Sulfate Radical Anion Formation in the Atmospheric Liquid Phase. *Environmental Science and Technology*, *49*(23), 13768–13776. https://doi.org/10.1021/acs.est.5b01658

Jimenez, J. L., Canagaratna, M. R., Donahue, N. M., Prevot, A. S. H., Zhang, Q., Kroll, J. H., et al. (2009). Evolution of organic aerosols in the atmosphere. *Science*, *326*(5959), 1525–1529. https://doi.org/10.1126/science.1180353

Kalalian, C., Abis, L., Depoorter, A., Lunardelli, B., Perrier, S., & George, C. (2020). Influence of indoor chemistry on the emission of mVOCs from Aspergillus niger molds. *Science of the Total Environment*, *741*, 140148. https://doi.org/10.1016/j.scitotenv.2020.140148

Kanakidou, M., Seinfeld, J. H., Pandis, S. N., Barnes, I., Dentener, F. J., Facchini, M. C., et al. (2005). Organic aerosol and global climate modelling: a review. *Atmospheric Chemistry and Physics*, *5*(4), 1053–1123. https://doi.org/10.5194/acp-5-1053-2005

Kaur, R., Hudson, B. M., Draper, J., Tantillo, D. J., & Anastasio, C. (2019). Aqueous reactions of organic triplet excited states with atmospheric alkenes. *Atmospheric Chemistry and Physics*, *19*(7), 5021–5032. https://doi.org/10.5194/acp-19-5021-2019

Kautzman, K. E., Surratt, J. D., Chan, M. N., Chan, A. W. H., Hersey, S. P., Chhabra, P. S., et al. (2010). Chemical composition of gas- and aerosol-phase products from the photooxidation of naphthalene. *Journal of Physical Chemistry A*, *114*(2), 913–934. https://doi.org/10.1021/jp908530s

Kroll, J. A., Frandsen, B. N., Kjaergaard, H. G., & Vaida, V. (2018). Atmospheric Hydroxyl Radical Source: Reaction of Triplet SO2 and Water. *Journal of Physical Chemistry A*, *122*(18), 4465–4469. https://doi.org/10.1021/acs.jpca.8b03524

Kuang, B. Y., Yeung, H. S., Lee, C. C., Griffith, S. M., & Yu, J. Z. (2018). Aromatic formulas in ambient PM2.5 samples from Hong Kong determined using FT-ICR ultrahigh-resolution mass spectrometry. *Analytical and Bioanalytical Chemistry*, *410*(24), 6289–6304. https://doi.org/10.1007/s00216-018-1239-8

Lee, H. J., Aiona, P. K., Laskin, A., Laskin, J., & Nizkorodov, S. A. (2014). Effect of solar radiation on the optical properties and molecular composition of laboratory proxies of atmospheric

brown carbon. *Environmental Science and Technology*, *48*(17), 10217–10226. https://doi.org/10.1021/es502515r

Li, S., Jiang, X., Roveretto, M., George, C., Liu, L., Jiang, W., et al. (2019a). Photochemical aging of atmospherically reactive organic compounds involving brown carbon at the air–aqueous interface. *Atmospheric Chemistry and Physics*, *19*(15), 9887–9902. https://doi.org/10.5194/acp-19-9887-2019

Li, Z., Tikkanen, O. P., Buchholz, A., Hao, L., Kari, E., Yli-Juuti, T., & Virtanen, A. (2019b). Effect of Decreased Temperature on the Evaporation of α-Pinene Secondary Organic Aerosol Particles. *ACS Earth and Space Chemistry*, *3*(12), 2775–2785. https://doi.org/10.1021/acsearthspacechem.9b00240

Lin, P., Rincon, A. G., Kalberer, M., & Yu, J. Z. (2012). Elemental composition of HULIS in the Pearl River Delta Region, China: Results inferred from positive and negative electrospray high resolution mass spectrometric data. *Environmental Science and Technology*, *46*(14), 7454–7462. https://doi.org/10.1021/es300285d

De Lucas, N. C., Ruis, C. P., Teixeira, R. I., Marçal, L. L., Garden, S. J., Corrêa, R. J., et al. (2014). Photosensitizing properties of triplet furano and pyrano-1,2- naphthoquinones. *Journal of Photochemistry and Photobiology A: Chemistry*, *276*, 16–30. https://doi.org/10.1016/j.jphotochem.2013.11.010

LuValle, J. E. (1952). The Reaction of Quinone and Sulfite. I. Intermediates. *Journal of the American Chemical Society*, *74*(12), 2970–2977. https://doi.org/10.1021/ja01132a005

Malecha, K. T., & Nizkorodov, S. A. (2016). Photodegradation of Secondary Organic Aerosol Particles as a Source of Small, Oxygenated Volatile Organic Compounds. *Environmental Science and Technology*, *50*(18), 9990–9997. https://doi.org/10.1021/acs.est.6b02313

Malecha, K. T., & Nizkorodov, S. A. (2017). Feasibility of Photosensitized Reactions with Secondary Organic Aerosol Particles in the Presence of Volatile Organic Compounds. *Journal of Physical Chemistry A*, *121*(26), 4961–4967. https://doi.org/10.1021/acs.jpca.7b04066

Manfrin, A., Nizkorodov, S. A., Malecha, K. T., Getzinger, G. J., McNeill, K., & Borduas-Dedekind, N. (2019). Reactive Oxygen Species Production from Secondary Organic Aerosols: The Importance of Singlet Oxygen. *Environmental Science and Technology*, *53*(15), 8553–8562. research-article. https://doi.org/10.1021/acs.est.9b01609

Martins-Costa, M. T. C., Anglada, J. M., Francisco, J. S., & Ruiz-López, M. F. (2018). Photochemistry of SO2 at the Air-Water Interface: A Source of OH and HOSO Radicals. *Journal of the American Chemical Society*, *140*(39), 12341–12344. https://doi.org/10.1021/jacs.8b07845

McNeill, K., & Canonica, S. (2016). Triplet state dissolved organic matter in aquatic photochemistry: Reaction mechanisms, substrate scope, and photophysical properties. *Environmental Science: Processes and Impacts*, *18*(11), 1381–1399. https://doi.org/10.1039/c6em00408c

McWhinney, R. D., Zhou, S., & Abbatt, J. P. D. (2013). Naphthalene SOA: Redox activity and naphthoquinone gas-particle partitioning. *Atmospheric Chemistry and Physics*, *13*(19), 9731–9744. https://doi.org/10.5194/acp-13-9731-2013

Monge, M. E., Rosenørn, T., Favez, O., Müller, M., Adler, G., Riziq, A. A., et al. (2012). Alternative pathway for atmospheric particles growth. *Proceedings of the National Academy of Sciences of the United States of America*, *109*(18), 6840–6844. https://doi.org/10.1073/pnas.1120593109

Nel, A. (2005). ATMOSPHERE: Enhanced: Air Pollution-Related Illness: Effects of Particles. *Science*, *308*(5723), 804–806. https://doi.org/10.1126/science.1108752

Oda, J., Nomura, S., Yasuhara, A., & Shibamoto, T. (2001). Mobile sources of atmospheric polycyclic aromatic hydrocarbons in a roadway tunnel. *Atmospheric Environment*, *35*(28), 4819–4827. https://doi.org/10.1016/S1352-2310(01)00262-X

Olson, T. M., & Hoffmann, M. R. (1989). Hydroxyalkylsulfonate formation: Its role as a S(IV) reservoir in atmospheric water droplets. *Atmospheric Environment (1967)*, *23*(5), 985–997. https://doi.org/10.1016/0004-6981(89)90302-8

Osburn, C. L., & Morris, D. P. (2003). Photochemistry of chromophoric dissolved organic matter in natural waters. In E. W. Helbling & H. Zagarese (Eds.), *UV Effects in Aquatic Organisms and Ecosystems* (Vol. 1, pp. 185–218). The Royal Society of Chemistry. https://doi.org/10.1039/9781847552266-00185

Riva, M., Robinson, E. S., Perraudin, E., Donahue, N. M., & Villenave, E. (2015). Photochemical aging of secondary organic aerosols generated from the photooxidation of polycyclic aromatic hydrocarbons in the gas-phase. *Environmental Science and Technology*, *49*(9), 5407–5416. https://doi.org/10.1021/acs.est.5b00442

Rossignol, S., Aregahegn, K. Z., Tinel, L., Fine, L., Nozière, B., & George, C. (2014). Glyoxal induced atmospheric photosensitized chemistry leading to organic aerosol growth. *Environmental Science and Technology*, *48*(6), 3218–3227. https://doi.org/10.1021/es405581g

Sarangi, B., Aggarwal, S. G., Sinha, D., & Gupta, P. K. (2016). Aerosol effective density measurement using scanning mobility particle sizer and quartz crystal microbalance with the estimation of involved uncertainty. *Atmospheric Measurement Techniques*, *9*(3), 859–875. https://doi.org/10.5194/amt-9-859-2016

Saukko, E., Lambe, A. T., Massoli, P., Koop, T., Wright, J. P., Croasdale, D. R., et al. (2012). Humidity-dependent phase state of SOA particles from biogenic and anthropogenic precursors. *Atmospheric Chemistry and Physics*, *12*(16), 7517–7529. https://doi.org/10.5194/acp-12-7517-2012

Saxena, P., & Seigneur, C. (1987). On the oxidation of SO2 to sulfate in atmospheric aerosols. *Atmospheric Environment (1967)*, *21*(4), 807–812. https://doi.org/10.1016/0004-6981(87)90077-1

Slade, J. H., Shiraiwa, M., Arangio, A., Su, H., Pöschl, U., Wang, J., & Knopf, D. A. (2017). Cloud droplet activation through oxidation of organic aerosol influenced by temperature and particle phase state. *Geophysical Research Letters*, *44*(3), 1583–1591. https://doi.org/10.1002/2016GL072424

Smith, J. D., Sio, V., Yu, L., Zhang, Q., & Anastasio, C. (2014). Secondary organic aerosol production from aqueous reactions of atmospheric phenols with an organic triplet excited state. *Environmental Science and Technology*, *48*(2), 1049–1057. https://doi.org/10.1021/es4045715

Sudakin, D. L., Stone, D. L., & Power, L. (2011). Naphthalene mothballs: Emerging and recurring issues and their relevance to environmental health. *Current Topics in Toxicology*, *7*(541), 13–19.

Tsui, W. G., Rao, Y., Dai, H. L., & McNeill, V. F. (2017). Modeling Photosensitized Secondary Organic Aerosol Formation in Laboratory and Ambient Aerosols. *Environmental Science and Technology*, *51*(13), 7496–7501. https://doi.org/10.1021/acs.est.7b01416

Wang, S., Zhou, S., Tao, Y., Tsui, W. G., Ye, J., Yu, J. Z., et al. (2019). Organic Peroxides and Sulfur Dioxide in Aerosol: Source of Particulate Sulfate. *Environmental Science and Technology*, *53*(18), 10695–10704. https://doi.org/10.1021/acs.est.9b02591

Wang, X., Hayeck, N., Brüggemann, M., Yao, L., Chen, H., Zhang, C., et al. (2017). Chemical

Characteristics of Organic Aerosols in Shanghai: A Study by Ultra-High-Performance Liquid Chromatography Coupled with Orbitrap Mass Spectrometry. *Journal of Geophysical Research: Atmospheres*, 1–20. https://doi.org/10.1002/2017JD026930

Wang, X., Gemayel, R., Hayeck, N., Perrier, S., Charbonnel, N., Xu, C., et al. (2020a). Atmospheric Photosensitization: A New Pathway for Sulfate Formation. *Environmental Science & Technology*, *54*(6), 3114–3120. https://doi.org/10.1021/acs.est.9b06347

Wang, X., Hayeck, N., Brüggemann, M., Abis, L., Riva, M., Lu, Y., et al. (2020b). Chemical Characteristics and Brown Carbon Chromophores of Atmospheric Organic Aerosols Over the Yangtze River Channel: A Cruise Campaign. *Journal of Geophysical Research: Atmospheres*, *125*(16), 1–13. https://doi.org/10.1029/2020JD032497

Wang, X. K., Rossignol, S., Ma, Y., Yao, L., Wang, M. Y., Chen, J. M., et al. (2016). Molecular characterization of atmospheric particulate organosulfates in three megacities at the middle and lower reaches of the Yangtze River. *Atmospheric Chemistry and Physics*, *16*(4), 2285–2298. https://doi.org/10.5194/acp-16-2285-2016

Wang, Y., Zhang, Q., Jiang, J., Zhou, W., Wang, B., He, K., et al. (2014). Key Role of Nitrate in Phase Transitions of Urban Particles: Implications of Important Reactive Surfaces for Secondary Aerosol Formation. *Journal of Geophysical Research: Atmospheres*, 425–440. https://doi.org/10.1002/2013JD021426.Received

Watne, Å. K., Psichoudaki, M., Ljungström, E., Le Breton, M., Hallquist, M., Jerksjö, M., et al. (2018). Fresh and Oxidized Emissions from In-Use Transit Buses Running on Diesel, Biodiesel, and CNG. *Environmental Science and Technology*, *52*(14), 7720–7728. https://doi.org/10.1021/acs.est.8b01394

Wilson, J., Imre, D., Beránek, J., Shrivastava, M., & Zelenyuk, A. (2015). Evaporation kinetics of laboratory-generated secondary organic aerosols at elevated relative humidity. *Environmental Science and Technology*, *49*(1), 243–249. https://doi.org/10.1021/es505331d

Wong, J. P. S., Zhou, S., & Abbatt, J. P. D. (2015). Changes in secondary organic aerosol composition and mass due to photolysis: Relative humidity dependence. *Journal of Physical Chemistry A*, *119*(19), 4309–4316. https://doi.org/10.1021/jp506898c

Yao, M., Zhao, Y., Hu, M., Huang, D., Wang, Y., Yu, J. Z., & Yan, N. (2019). Multiphase Reactions between Secondary Organic Aerosol and Sulfur Dioxide: Kinetics and Contributions to Sulfate Formation and Aerosol Aging. *Environmental Science and Technology Letters*, *6*(12), 768–774. https://doi.org/10.1021/acs.estlett.9b00657

Ye, J., Abbatt, J. P. D., & Chan, A. W. H. (2018a). Novel pathway of SO2 oxidation in the atmosphere: reactions with monoterpene ozonolysis intermediates and secondary organic aerosol. *Atmospheric Chemistry and Physics*, *18*(8), 5549–5565. https://doi.org/10.5194/acp-18-5549-2018

Ye, Q., Robinson, E. S., Ding, X., Ye, P., Sullivan, R. C., & Donahue, N. M. (2016). Mixing of secondary organic aerosols versus relative humidity. *Proceedings of the National Academy of Sciences of the United States of America*, *113*(45), 12649–12654. https://doi.org/10.1073/pnas.1604536113

Ye, Q., Upshur, M. A., Robinson, E. S., Geiger, F. M., Sullivan, R. C., Thomson, R. J., & Donahue, N. M. (2018b). Following Particle-Particle Mixing in Atmospheric Secondary Organic Aerosols by Using Isotopically Labeled Terpenes. *Chem*, *4*(2), 318–333. https://doi.org/10.1016/j.chempr.2017.12.008

Yli-Juuti, T., Pajunoja, A., Tikkanen, O. P., Buchholz, A., Faiola, C., Väisänen, O., et al. (2017). Factors controlling the evaporation of secondary organic aerosol from α-pinene ozonolysis. *Geophysical Research Letters*, *44*(5), 2562–2570. https://doi.org/10.1002/2016GL072364

Yu, L., Smith, J., Laskin, A., Anastasio, C., Laskin, J., & Zhang, Q. (2014). Chemical characterization of SOA formed from aqueous-phase reactions of phenols with the triplet excited state of carbonyl and hydroxyl radical. *Atmospheric Chemistry and Physics*, *14*(24), 13801–13816. https://doi.org/10.5194/acp-14-13801-2014

Zhang, Q., Jimenez, J. L., Canagaratna, M. R., Allan, J. D., Coe, H., Ulbrich, I., et al. (2007). Ubiquity and dominance of oxygenated species in organic aerosols in anthropogenically-influenced Northern Hemisphere midlatitudes. *Geophysical Research Letters*, *34*(13), 1–6. https://doi.org/10.1029/2007GL029979

Zhang, Z., Lin, L., & Wang, L. (2012). Atmospheric oxidation mechanism of naphthalene initiated by OH radical. A theoretical study. *Physical Chemistry Chemical Physics*, *14*(8), 2645–2650. https://doi.org/10.1039/c2cp23271e

Figures

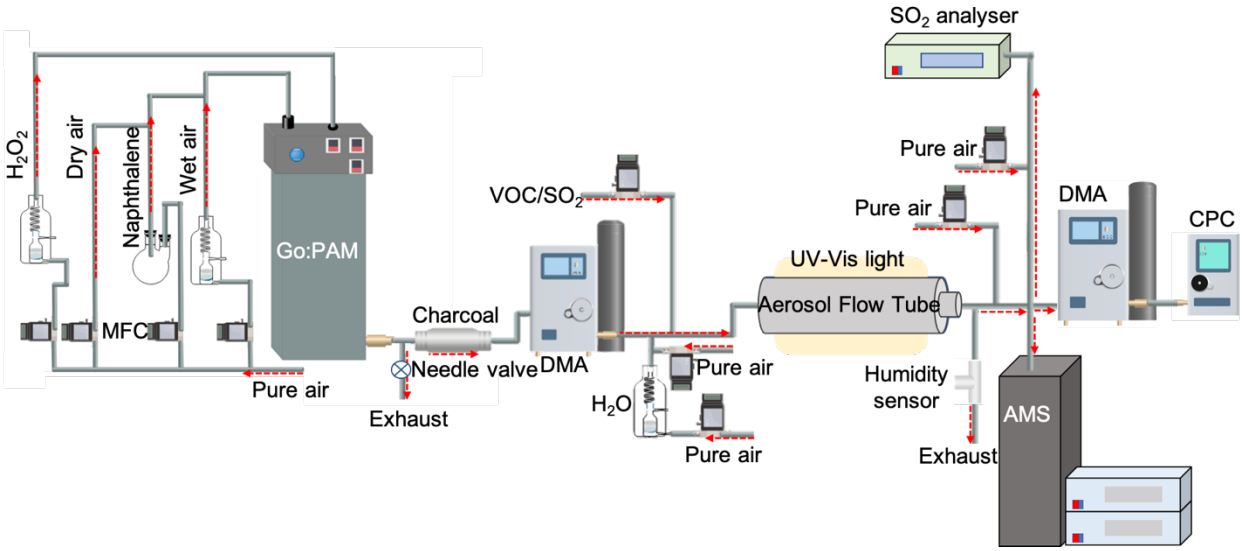

Figure 1. Schematic of the experimental setup with the Go:PAM flow and aerosol flow reactors.

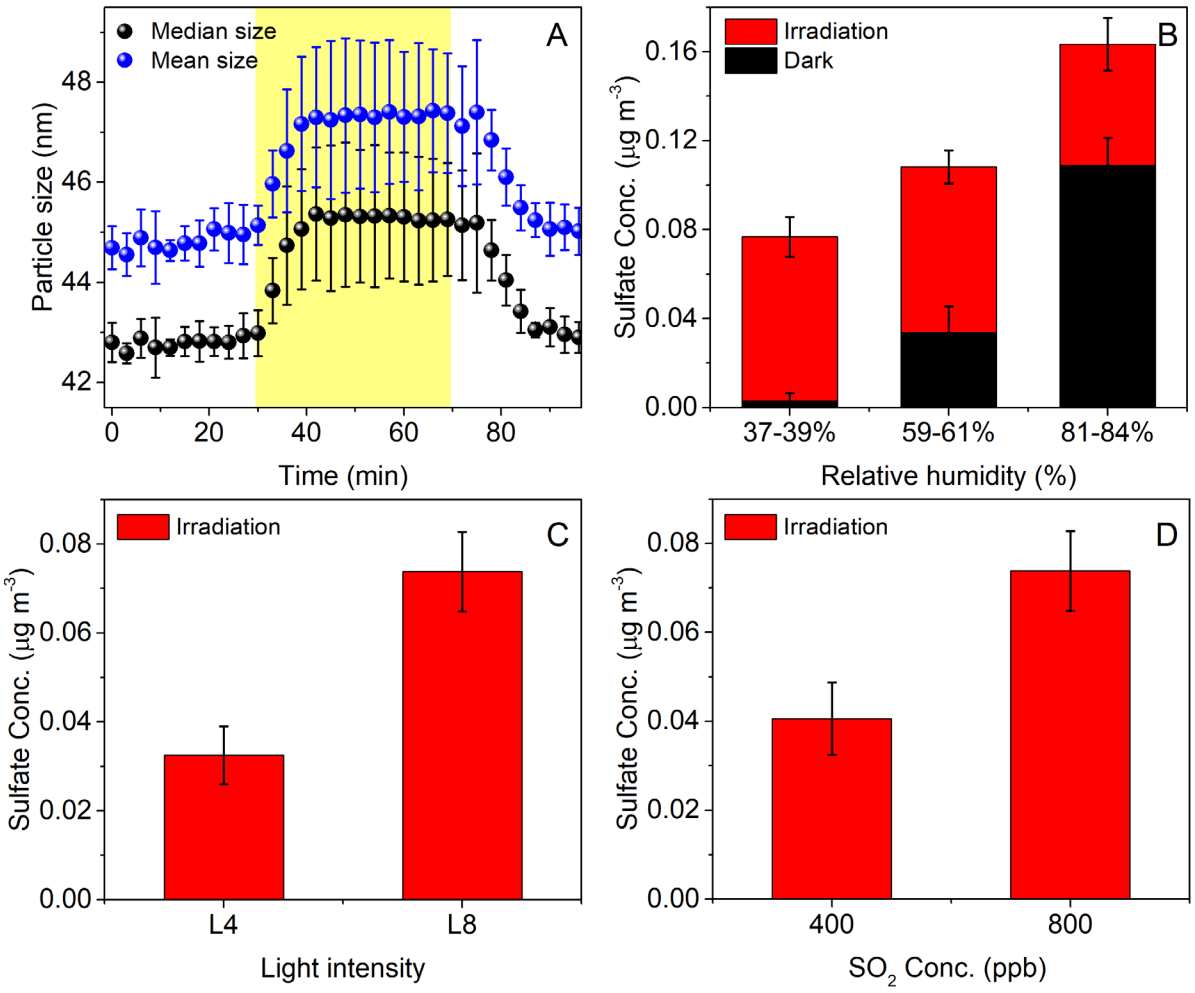

Figure 2. Median and mean diameter (± 2σ) growths of naphthalene-derived SOA exposed to UV light and SO_2 for 16 min in the AFT (A). The yellow region corresponds to the irradiation time. Sulfate production as measured by the cTOF-AMS of naphthalene-derived SOA exposed to SO_2 at different RH (B), under different light intensities (C), and with different SO_2 concentrations (D). L4 means four lamps were turned on; and L8 means eight lamps were turned on.

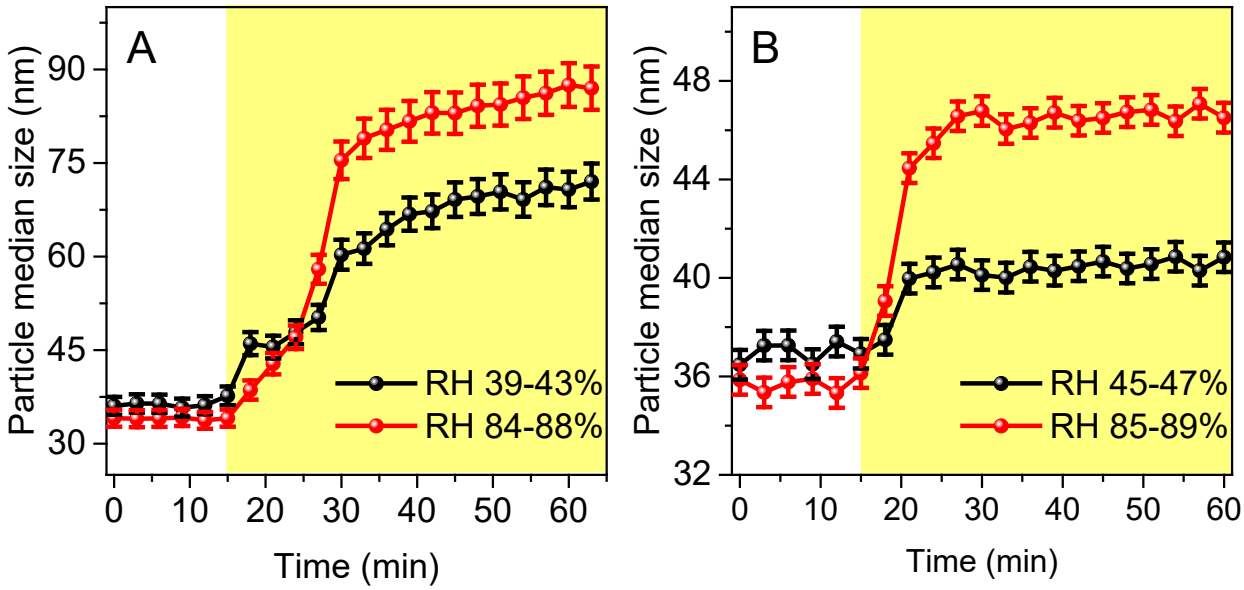

576

577 **Figure 3.** Median diameter (± 2σ) growths of Nap-derived SOA exposed to UV-A light and 0.1
578 ppm d-limonene (A) and 0.8 ppm β-pinene for 30 min in the AFT. The yellow region corresponds
579 to the irradiation time.

580

581

582

583

584

585

586

587

588 **Table 1.** Median Diameter Growth Factor (DGF, %) of naphthalene-derived SOA with different
589 gaseous compounds and RH. Dp_0, initial particle median diameter; Dp, particle median diameter
590 after irradiation.

Gaseous compounds	Concentration (ppm)	Residence time (min)	RH	Dp_0 (nm)	Dp (nm)	**DGF (%)**
None	0	16	47-49%	44.1±0.2	43.5±0.3	**-1.4**
	0	16	68-71%	43.8±0.3	42.2±0.4	**-3.8**
	0	16	85-89%	42.4±0.2	41.4±0.3	**-2.4**
SO_2	1	16	40-43%	44.8±0.2	43.0±0.3	**-4.2**
	1	16	61-65%	42.5±0.2	41.3±0.8	**-2.9**
	1	16	86-90%	42.8±0.4	44.7±0.7	**4.3**
	0.7	16	86-90%	42.9±0.2	43.9±0.2	**2.3**
	0.4	16	86-90%	42.9±0.2	43.1±0.2	**0.5**
d-Limonene	0.1	25	39-43%	36.4±0.7	71.4±1.3	**50.8**
	0.1	25	84-88%	34.0±0.2	85.4±1.6	**58.7**
β-pinene	0.8	25	45-47%	37.0±0.4	40.6±0.3	**8.9**
	0.8	25	85-89%	35.7±0.3	47.1±0.3	**24.2**

591